arXiv:0908.4145v1 [q-bio.MN] 28 Aug 2009

Modeling of the genetic switch of bacteriophage TP901-1: A heteromer of CI and MOR ensures robust bistability

Hiizu Nakanishi[a], Margit Pedersen[b], Anne K. Alsing[b], and Kim Sneppen[b]

[a]*Department of Physics, Kyushu University 33, Fukuoka 812-8581, Japan*
[b]*Center for Models of Life, Niels Bohr Institute, University of Copenhagen, Blegdamsvej 17, DK-2100 Copenhagen, Denmark*

Abstract

The lytic-lysogenic switch of the temperate lactococcal phage TP901-1 is fundamentally different from that of phage lambda. In phage TP901-1, the lytic promoter P_L is repressed by CI whereas repression of the lysogenic promoter P_R requires the presence of both of the antagonistic regulator proteins, MOR and CI. We model the central part of the switch and compare the two cases for P_R repression: the one where the two regulators interact only on the DNA, and the other where the two regulators form a heteromer complex in the cytoplasm prior to DNA binding. The models are analyzed for bistability, and the predicted promoter repression folds are compared to experimental data. We conclude that the experimental data are best reproduced the latter case, where a heteromer complex forms in solution. We further find that CI sequestration by the formation of MOR:CI complexes in cytoplasm makes the genetic switch robust.

Key words:
temperate bacteriophage TP901-1, genetic switch, mixed feedback loop, sequestration, protein interaction

---

1. Introduction

Phenotypic variability under homogeneous conditions can readily be obtained by interlinking multiple gene regulatory pathways. Several well-characterized examples of phenotypic variations are known to be important for different developmental process of bacteria, such as the presence of persister cells in *Staphylococcus aureus* and *E. coli*, development of natural competence and sporulation in *Bacillus subtilis*, and the choice between lytic or lysogenic growth of temperate bacteriophages [1, 2]. Two distinguishable phenotypes may originate from a bistable system, i.e. a system that can toggle between two alternative stable steady-states [3]. Infection of bacteria by temperate bacteriophages provides a classical example of the possibility to choose between two alternative modes of development.

The bacteriophage lambda infecting *Escherichia coli* has been subjected to decades of intensive study, making the lytic-lysogenic switch one of the best understood gene regulatory systems[4, 5, 6]. The bistability of the lambda switch is obtained from a double negative feedback mechanism, where two repressor proteins directly repress transcription of the other repressor gene. This system has a stable state with one promoter on and the other off, and vice versa for the other stable state. Once either state has been established, it would persist indefinitely or until some trigger stimulus forces the system to switch to the other state.

The genetic switch of the temperate lactococcal bacteriophage TP901-1 infecting *Lactococcus lactis* subsp. *cremoris* provides a regulatory system diverse from the lambda genetic switch. A previous study has demonstrated that a DNA fragment obtained from the temperate lactococcal phage TP901-1 shows bistability when introduced into *Lactococcus lactis*. The cloned DNA fragment contains the two divergently oriented promoters, P_R and P_L, and the two promoter proximal genes *cI* and *mor* [7](Fig.1a). A knockout mutation in the *mor* gene showed that CI ensures tight repression of the P_L promoter and partially repression of the P_R promoter whereas a knockout mutation in the *cI* gene results in open states of both P_R and P_L, showing that MOR by itself does not exhibit repression of either promoter[8, 9]. Two types of repression has been shown: i) *MOR-independent repression*, which is responsible for repression of P_L. The P_L promoter is repressed by cooperative binding of CI to the three operator sites O_R, O_L and O_D, by the formation of a CI-DNA loop structure. ii) *MOR-dependent repression*, which is responsible for repres-

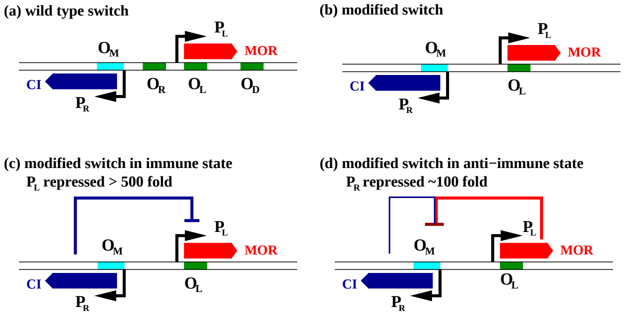
(a) wild type switch
(b) modified switch
(c) modified switch in immune state
P_L repressed > 500 fold
(d) modified switch in anti−immune state
P_R repressed ~100 fold
O_M
P_L
MOR
CI
P_R
O_R
O_L
O_D

Figure 1: The regulatory circuit of the genetic switch from phage TP901-1 may be described as a double negative regulatory network. (a) Wild type genetic switch with O_L, O_R, and O_D sites. The relative positions of the *cI* and *mor* genes and the divergently oriented promoters P_R and P_L are also shown. The cyan box represents a putative O_M site. (b) Modified switch investigated in this paper. Only one CI operator site, O_L, is present (dark green box). (c) Immune state of the modified switch. CI represses transcription from P_L approximately 1000-fold by binding to the O_L operator site with transcription from P_R being allowed. (d) Anti-immune state of the modified switch. Repression of P_R depends on both CI and MOR, which repress transcription from P_R approximately 100-fold with transcription from P_L being allowed.

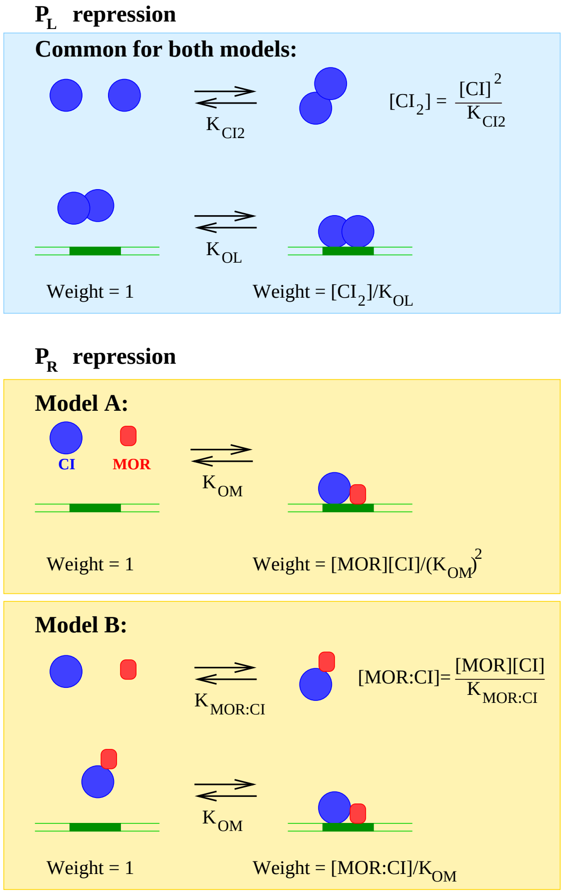

Figure 2: Repression of P_L though binding of CI_2 at O_L is employed in both models (blue box). Repression of P_R is supposed to occur by direct binding of CI and MOR to O_M (Model A) or by formation of a MOR:CI complex prior to binding to O_M (Model B). The statistical weight is given for the different states of the operator sites. In Model A, it is assumed that binding of CI alone to O_M is so week that the operator is only occupied when binding is stabilized by MOR, or vice versus if MOR binds first.

sion of P_R and only occurs in the presence of both MOR and CI. This repression is suggested to occur through MOR and CI binding at a putative O_M operator site [9]. Hence, the bistability of the genetic switch from phage TP901-1 may be described as a mixed feedback loop, where both of the antagonistic repressor proteins are involved in P_R repression. It is still not clear how MOR and CI collectively repress transcription from P_R, and so far there is no direct experimental evidence for interaction between CI and MOR.

In order to understand the mechanism of switching in phage TP901-1, we here study a modified version of the cloned wild-type TP901-1 switch(Fig.1b). This construct contains only one of the three CI operator sites, O_L, which gives tight repression of P_L thus still sustains the bistable behavior of the construct. In the immune state, the P_L promoter is repressed approximately 1,000-fold, but high expression from P_R is allowed due to the absence of O_R, that autoregulates transcription from P_R in the case of the wild-type switch [9] (Fig.1c). In the anti-immune state, P_R is repressed approximately 100-fold but high expression from P_L is allowed[9] (Fig.1d).

Generally speaking, it is not easy to predict the behavior of a bistable switch without quantitative analysis because a bistable switch is a dynamical and highly nonlinear system. In the present case of TP901-1, even the modified version of the switch (Fig.1b) could involve a number of mechanisms, such as cooperativity binding via homo/hetero-dimerization, sequestration via heterodimerization, intertwined loops of negative and positive feed back via protein interactions, etc. In such a situation, the only way to obtain any reliable results is to perform quantitative analysis on specific models. By confronting numerical results with experimental data, we can restrict possible mechanisms with plausible parameters

In this paper, we construct mathematical models for this modified bistable system based upon statistical mechanics, examine their behavior in the steady states numerically, and compare the obtained repression folds with experimental observations[9]. We assume that P_L is repressed by the CI dimer binding to the operator O_L since the operator has two inverted repeated sequences [10]. On the other hand, the MOR-dependent repression of P_R is assumed to be brought about by the MOR:CI:DNA complex formation at the putative O_M operator. Since the amino sequence of MOR shows high similarity to the DNA-binding Helix-turn-Helix domain of the repressor protein encoded by *Escherichia coli* phage 434 [11] MOR is likely to be a DNA binding protein, but the fact that MOR alone does not repress transcription from either P_L or P_R suggests that the DNA-binding affinity of MOR is negligible. CI alone does not repress P_R in this system due to absence of O_R operator. Based upon these observations, we test two different scenarios for P_R repression(Fig.2): i) repression through direct binding of CI and MOR to O_M (Model A), and ii) repression through binding of MOR:CI complex to O_M with the complex being formed in the cytoplasm prior to the binding to DNA (Model B).

The MOR:CI:DNA complex formation in Model A may be regarded as an extreme case of Model B where the MOR:CI complex formation in cytoplasm is so weak that the complex is stabilized only when it binds to DNA, thus there is no substantial presence of MOR:CI complex in the cytoplasm. However, distinguishing Model A from Model B helps us to recognize two distinct aspects in the P_R repression by the MOR:CI:DNA complex, i.e., co-operativity and sequestration; The latter has been studied in silico as a possible mechanism for a genetic switch[12, 13] and demonstrated to provide strong nonlinearity[14, 15]. In fact, our Model B is a reminiscent of one of the bistable switches obtained by the simulated evolution (Fig.3A in [12]). We will demonstrate that CI sequestration by the MOR:CI formation in cytoplasm can make a robust bistable system and is actually a plausible switching mechanism for TP901-1.

Theory

The regulatory circuit in the present system consists of the two promoters P_L and P_R, which produce MOR and CI, respectively(Fig.1b). The promoter P_L is repressed by CI binding at O_L, thus the P_L activity is given by a function of the CI concentration as

$$pL([\mathrm{CI}]) = pL_0 \cdot f_{\mathrm{OL}}([\mathrm{CI}]), \tag{1}$$

where pL_0 is the bare activity of the promoter P_L. The function $f_{\mathrm{OL}}([\mathrm{CI}])$ represents the repression factor. In the absence of CI, there is no repression: $f_{\mathrm{OL}}(0) = 1$. The P_R activity, on the other hand, depends on the concentrations of both CI and MOR. Accordingly, the P_R activity can be written as

$$pR([\mathrm{MOR}], [\mathrm{CI}]) = pR_0 \cdot f_{\mathrm{OM}}([\mathrm{MOR}], [\mathrm{CI}]) \tag{2}$$

with pR_0 being the bare activity. The function $f_{\mathrm{OM}}([\mathrm{MOR}], [\mathrm{CI}])$ is the repression factor due to the binding of MOR and CI at O_M, and satisfies $f_{\mathrm{OM}}(0, [\mathrm{CI}]) = f_{\mathrm{OM}}([\mathrm{MOR}], 0) = 1$.

The promoter P_L produces MOR, and P_R produces CI, thus in the modeled feedback system, the total concentration for each protein, $[\mathrm{MOR}]_{\mathrm{total}}$ and $[\mathrm{CI}]_{\mathrm{total}}$, is governed by the dynamics equations,

$$\frac{d}{dt}[\mathrm{MOR}]_{\mathrm{total}} = \frac{1}{\tau_M}\Big(pL([\mathrm{CI}]) - [\mathrm{MOR}]_{\mathrm{total}}\Big), \tag{3}$$

$$\frac{d}{dt}[\mathrm{CI}]_{\mathrm{total}} = \frac{1}{\tau_C}\Big(pR([\mathrm{MOR}], [\mathrm{CI}]) - [\mathrm{CI}]_{\mathrm{total}}\Big), \tag{4}$$

where τ_M and τ_C are the degradation times for MOR and CI, respectively. To simplify the notation, we have rescaled the promoter activities, Eqs.(1) and (2), by the degradation times, i.e. the promoter activities are now measured in terms of the steady state protein concentrations.

In steady states, the production and the degradation of each protein should balance, therefore, the promoter activities and the concentrations of the expressed proteins in the cytoplasm should satisfy *the steady state condition*,

$$\begin{aligned} pL([\mathrm{CI}]) &= [\mathrm{MOR}]_{\mathrm{total}}, & (5)\\ pR([\mathrm{MOR}], [\mathrm{CI}]) &= [\mathrm{CI}]_{\mathrm{total}}. & (6) \end{aligned}$$

Not all steady states are stable against small perturbations. A steady state is unstable if a perturbation drives the system out of the state; The stability should be determined by the dynamics equations, Eqs.(3) and (4) (See supplementary material). If there are two stable steady states, the system shows bistability.

We assume that the repression factors, f_{OL} and f_{OM} in Eqs.(1) and (2), are given by the statistical weights at equilibrium that the corresponding operators are not bound by the regulators. This approximation holds when the time that RNA polymerase (RNAP) needs to start elongation after binding to DNA is much shorter than the time scales of binding/unbinding of RNAP and repression factors to the promoter/operator sites [16]. The equilibrium statistical weights depend upon the repressor concentrations, and their dependence is characterized by the Hill coefficient and the affinities of the repressors to the operator sites [17, 18, 19].

For *the MOR-independent repression of P_L*, we suppose that P_L is repressed by CI dimer binding at O_L, and that the dimers are formed in the cytoplasm before binding. Thus, within the above approximation for the repression factor, the $\mathrm{P_L}$ activity is given by

$$pL([\mathrm{CI}]) = pL_0 \cdot \frac{1}{1 + [\mathrm{CI}_2]/K_{\mathrm{OL}}}, \tag{7}$$

where the affinity K_{OL} represents the CI_2 concentration at which $\mathrm{O_L}$ is occupied for 50% of the time. Since the dimer concentration $[\mathrm{CI}_2]$ is related to the monomer concentration [CI] as

$$[\mathrm{CI}_2] = \frac{[\mathrm{CI}]^2}{K_{\mathrm{CI}_2}} \tag{8}$$

with the dissociation constant K_{CI_2}, Eq.(7) may be written as

$$pL([\mathrm{CI}]) = pL_0 \cdot \frac{1}{1 + [\mathrm{CI}]^2/\tilde{K}^2_{\mathrm{OL}}} \tag{9}$$

with the effective affinity

$$\tilde{K}_{\mathrm{OL}} \equiv \sqrt{K_{\mathrm{CI}_2} K_{\mathrm{OL}}} \tag{10}$$

for CI concentration. In Fig.3, the activity of $\mathrm{P_L}$ as a function of [CI] is plotted by a green line.

As for *the MOR-dependent repression of* $\mathrm{P_R}$, we will examine two models. In Model A, monomers of MOR and CI may bind cooperatively at $\mathrm{O_M}$, but we do not assume any MOR:CI complexes formed in cytoplasm before binding to DNA. In Model B, on the other hand, CI and MOR may associate in cytoplasm before they bind at $\mathrm{O_M}$. For both models, $\mathrm{P_R}$ is repressed by the formation of the MOR:CI:DNA complex at $\mathrm{O_M}$. The important point in Model B is that *the formation of MOR:CI heteromers competes with CI dimer formation by sequestering CI monomers* .

Model A

We first consider a MOR:CI:DNA complex containing one MOR and one CI protein as illustrated in Fig.2. Then, we can approximate the total concentration of MOR unit by the MOR monomer concentration,

$$[\mathrm{MOR}]_{\mathrm{total}} = [\mathrm{MOR}]. \tag{11}$$

The activity of the $\mathrm{P_R}$ promoter is repressed from the bare activity pR_0 by the statistical weight that the operator $\mathrm{O_M}$ is not occupied by MOR and CI,

$$pR([\mathrm{MOR}],[\mathrm{CI}]) = pR_0 \, \frac{1}{1 + [\mathrm{MOR}][\mathrm{CI}]/(K_{\mathrm{OM}})^2} . \tag{12}$$

The affinity K_{OM} is the concentration $\sqrt{[\mathrm{MOR}]\cdot[\mathrm{CI}]}$ where $\mathrm{O_M}$ is occupied by MOR and CI for 50% of the time.

The steady state is determined from the steady state condition Eqs.(5) and (6) by eliminating the MOR concentrations. With the help of Eq.(11), we obtain

$$pR\Big(pL([\mathrm{CI}]),[\mathrm{CI}]\Big) \quad = \quad [\mathrm{CI}]_{\mathrm{total}}, \tag{13}$$

which represents the balance between the production and the degradation of CI. This can be solved graphically by plotting the both sides as a function of [CI],

$$\begin{aligned} &pR\Big(pL([\mathrm{CI}]),[\mathrm{CI}]\Big) \\ &\quad = \quad pR_0 \left[1 + \frac{pL_0\, \tilde{K}_{\mathrm{OL}}/(K_{\mathrm{OM}})^2}{([\mathrm{CI}]/\tilde{K}_{\mathrm{OL}}) + (\tilde{K}_{\mathrm{OL}}/[\mathrm{CI}])} \right]^{-1}, \end{aligned} \tag{14}$$

$$[\mathrm{CI}]_{\mathrm{total}} = [\mathrm{CI}] + 2\frac{[\mathrm{CI}]^2}{K_{\mathrm{CI}_2}}. \tag{15}$$

Eq.(14) represents the $\mathrm{P_R}$ activity in the system where MOR is provided by $\mathrm{P_L}$ but [CI] is controlled externally. Note that the relative strength of the bare promoters, pL_0 and pR_0, does not affect the system behaviors, such as bistability or repression folds, because there is no direct interaction between MOR and CI in this model.

Model B

In this model, a MOR CI heterodimer is formed in solution before it binds to the putative $\mathrm{O_M}$ site to repress $\mathrm{P_R}$ (Fig.2). The activity of the $\mathrm{P_L}$ promoter is again given by Eq.(9) but the $\mathrm{P_R}$ activity is

$$pR([\mathrm{MOR}],[\mathrm{CI}]) = pR_0 \, \frac{1}{1 + [\mathrm{MOR\ CI}]/K_{\mathrm{OM}}}, \tag{16}$$

where K_{OM} now represents the concentration of the MOR CI heterodimer at which $\mathrm{O_M}$ is occupied for 50% of the time. The concentration of the MOR CI heterodimer is given as

$$[\mathrm{MOR\ CI}] = \frac{[\mathrm{MOR}]\cdot[\mathrm{CI}]}{K_{\mathrm{MOR\ CI}}} \tag{17}$$

with the dissociation constant $K_{\mathrm{MOR\ CI}}$ for the heterodimer.

The formation of the heterodimers couples the monomer concentrations of CI and MOR through

$$\begin{aligned} [\mathrm{CI}]_{\mathrm{total}} \quad &= \quad [\mathrm{CI}] + 2[\mathrm{CI}_2] + [\mathrm{MOR\ CI}], & (18) \\ [\mathrm{MOR}]_{\mathrm{total}} \quad &= \quad [\mathrm{MOR}] + [\mathrm{MOR\ CI}], & (19) \end{aligned}$$

which leads to the competition between the CI_2 formation and the MOR CI formation. Note that $[\mathrm{CI}_2]$ is still given by Eq.(8).

The steady state is determined as in the case of Model A; We consider the $\mathrm{P_R}$ activity as a function of [CI] when MOR is provided by $\mathrm{P_L}$. From Eqs.(17) and (19), [MOR] is expressed in terms of [CI] and $[\mathrm{MOR}]_{\mathrm{total}}$,

$$[\mathrm{MOR}] = \frac{[\mathrm{MOR}]_{\mathrm{total}}}{1 + [\mathrm{CI}]/K_{\mathrm{MOR:CI}}}, \tag{20}$$

and then, in the steady state where Eq.(5) holds, $[\mathrm{MOR}]_{\mathrm{total}}$ is given by the $\mathrm{P_L}$ activity with Eq.(7). Then the steady state condition Eq.(6) for $\mathrm{P_R}$ becomes

$$pR\left(\frac{pL([\mathrm{CI}])}{1 + [\mathrm{CI}]/K_{\mathrm{MOR:CI}}}, [\mathrm{CI}]\right) = [\mathrm{CI}]_{\mathrm{total}}, \tag{21}$$

which can be solved graphically with the explicit forms for the both sides:

$$pR\left(\frac{pL([\mathrm{CI}])}{1 + [\mathrm{CI}]/K_{\mathrm{MOR:CI}}}, [\mathrm{CI}]\right) = pR_0\Bigg[1+ \frac{pL_0\, \tilde{K}_{\mathrm{OL}}/(\tilde{K}_{\mathrm{OM}})^2}{([\mathrm{CI}]/\tilde{K}_{\mathrm{OL}}) + (\tilde{K}_{\mathrm{OL}}/[\mathrm{CI}])} \cdot \frac{1}{1 + [\mathrm{CI}]/K_{\mathrm{MOR:CI}}}\Bigg]^{-1} \tag{22}$$

$$[\mathrm{CI}]_{\mathrm{total}} = [\mathrm{CI}] + 2\frac{[\mathrm{CI}]^2}{K_{\mathrm{CI_2}}} + pL([\mathrm{CI}])\,\frac{[\mathrm{CI}]/K_{\mathrm{MOR:CI}}}{1 + [\mathrm{CI}]/K_{\mathrm{MOR:CI}}}, \tag{23}$$

where the effective affinities are

$$\tilde{K}_{\mathrm{OM}} \equiv \sqrt{K_{\mathrm{MOR:CI}} \cdot K_{\mathrm{OM}}} \text{ and } \tilde{K}_{\mathrm{OL}} \equiv \sqrt{K_{\mathrm{CI_2}} K_{\mathrm{OL}}}. \tag{24}$$

Eq.(21) represents the balance between the production and degradation of CI in the system where MOR is provided by $\mathrm{P_L}$. Note that Model B reduces to Model A in the limit of large $K_{\mathrm{MOR:CI}}$ with $\tilde{K}_{\mathrm{OM}}$ being kept constant as has been discussed at the end of Introduction.

2. Results

We numerically examine the steady states for the two versions of the models we have constructed (Fig.2).

Model A

In our first model, we study the possibility for bistability in the system where $\mathrm{P_R}$ is repressed by binding a MOR monomer and a CI monomer to $\mathrm{O_M}$ without direct interaction between MOR and CI in the cytoplasm. The binding affinities for each of the proteins alone at $\mathrm{O_M}$ should be negligible because the $\mathrm{P_R}$ repression requires both of the proteins. Hence, the affinity K_{OM} in Eq.(12) may be considered as the effective binding affinity $\tilde{K}_{\mathrm{OM}}$ for MOR and CI with very weak MOR CI formation, or as the resulting binding affinities from CI:$\mathrm{O_M}$, MOR:$\mathrm{O_M}$, and the interaction between the bound proteins.

Figure 3 shows a typical example of the $\mathrm{P_L}$ activity of Eq.(9) (green line), the $\mathrm{P_R}$ activity of Eq.(14) (solid red line), and the total concentration of CI, or degradation rate, of Eq.(15) (dashed red line) as a function of free [CI] in the logarithmic scale. One can see that $\mathrm{P_L}$ (green line) is fully active and produces a lot of MOR at low [CI], whereas its activity is monotonically decreasing with increasing [CI], due to $\mathrm{P_L}$ repression by $\mathrm{CI_2}$ binding at $\mathrm{O_L}$; $\mathrm{P_L}$ is virtually shut down beyond $[\mathrm{CI}] \approx \tilde{K}_{\mathrm{OL}} = \sqrt{K_{CI_2} \cdot K_{\mathrm{OL}}} = 6 \cdot 10^{-4}$.

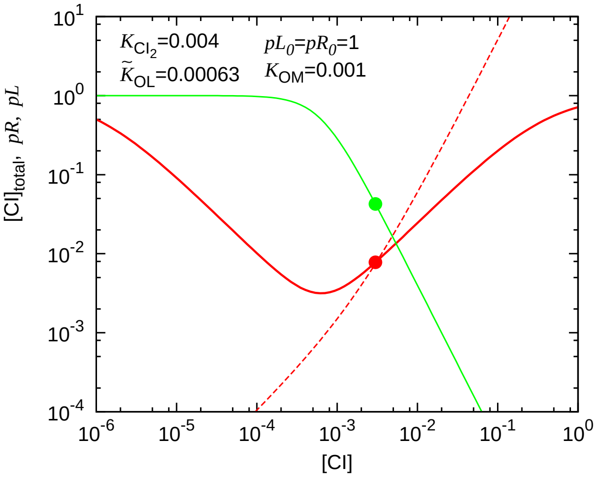

Figure 3: Model A. Promoter activities, pL and pR, and $[\mathrm{CI}]_{\mathrm{total}}$ as a function of free [CI]. Curves represent $\mathrm{P_L}$ activity of Eq.(9) (green line), $\mathrm{P_R}$ activity of Eq.(14) (solid red line), and $[\mathrm{CI}]_{\mathrm{total}}$ of Eq.(15)(dashed red line). The filled red circle at the intersection between the $[\mathrm{CI}]_{\mathrm{total}}$ and $\mathrm{P_R}$ curve represents the steady state.

On the other hand, the $\mathrm{P_R}$ activity (solid red line) shows a more complicated behavior, i.e., $\mathrm{P_R}$ is open both at very low and high [CI] concentrations but repressed at the intermediate concentration. One can understand this behavior by noting that the solid red line, Eq.(14), represents the $\mathrm{P_R}$ activity in the system where MOR is expressed from $\mathrm{P_L}$ under CI control; At low [CI], there is plenty of MOR due to high $\mathrm{P_L}$ activity, while at high [CI], no MOR is present. The $\mathrm{P_R}$ activity is repressed only at intermediate [CI] because both MOR and CI are necessary for its repression by means of the MOR:CI:DNA complex formation.

In the steady state, the production and the degradation of each protein should balance. Since CI is expressed from $\mathrm{P_R}$ and the degradation of CI is assumed to be proportional to the total concentration of CI, the steady states are identified as $pR(pL([\mathrm{CI}]), [\mathrm{CI}]) = [\mathrm{CI}]_{\mathrm{total}}$, namely, Eq.(13). We thus find the steady states at the intersection points between the pR and $[\mathrm{CI}]_{\mathrm{total}}$ curves represented by Eqs.(14) (solid red line) and (15) (red dashed line), respectively.

In Fig.3, only one intersection point is observed between the two curves, showing that there is only one steady state solution. This uniqueness of steady state holds true for any given value of the parameters, because the activity of P_R given by Eq.(14) never increases faster than proportional to CI, whereas $[\mathrm{CI}]_{\mathrm{total}}$ by Eq.(15) always increases faster or proportional to [CI]. Therefore, bistability is never realized in Model A with the assumption of binding of one MOR and one CI for repression of P_R.

Variant of Model A

Bistability may be obtained in Model A if a larger number of proteins are allowed to form a complex structure at O_M. Suppose m MOR monomers and c CI monomers bind at O_M to form the MOR_m:CI_c:DNA complex that represses transcription from P_R, then for the expression for the P_R activity, Eq.(12) should be replaced by

$$\begin{aligned} &pR([\mathrm{MOR}],[\mathrm{CI}]) \\ &\quad = \quad pR_0\,\frac{1}{1+[\mathrm{MOR}]^m[\mathrm{CI}]^c/(K_{\mathrm{OM}})^{m+c}}, \end{aligned} \qquad (25)$$

while all the other equations remain the same. Using this for the left hand side of the steady state equation (13) with $[\mathrm{MOR}] \propto 1/[\mathrm{CI}]^2$ from Eq.(7) for large [CI], one can see that the largest slope of the P_R activity as a function of [CI] is $2m-c$ in the logarithmic scale. Since the slope of the plot of $[\mathrm{CI}]_{\mathrm{total}}$ given by Eq.(15) is between 1 and 2, the steady state equation (13) can have more than two solutions with Eq.(25) when $2m-c \geq 2$. In the case of $m = 2$, we could obtain multiple solutions with $c = 1$ or 2, i.e., two MOR monomers binding together with one or two CI monomers at O_M. Examples for Model A with $(m,c) = (2,1)$ and $(2,2)$ are shown in Fig. 4. In each example, the intersections between the solid red line (the P_R activity) and the dashed red line (the total CI concentration) represent steady state solutions. One can see there are three solutions for each case in Fig.4.

Dynamical analysis shows that the steady state in the middle marked by an open red circle is unstable against small fluctuations, and the states at the ends marked by filled red circles are stable (See supplementary material for detail). Full analysis requires Eqs.(3) and (4), but the stability may be understood in the following way; For the steady state in the middle, if the CI monomer concentration increases by fluctuation from the steady value of [CI], the CI production from P_R will increase more than the increase in degradation given by $[\mathrm{CI}]_{\mathrm{total}}$, as is seen in Fig.4, where the solid red line of the P_R activity goes above the dashed red line of $[\mathrm{CI}]_{\mathrm{total}}$, upon increasing [CI] from the middle steady state. This means that such a fluctuation causes further increases of [CI], consequently, the state is driven out of the steady state. On the other hand, the steady states at both ends represent stable states. A fluctuation towards larger [CI] leads to insufficient CI production in comparison with the CI degradation, i.e. the solid red line goes under the dashed red line as [CI] increases. This brings the system back to the original state, therefore, they are stable. Thus, the system has two stable steady states, which leads to bistability.[1]

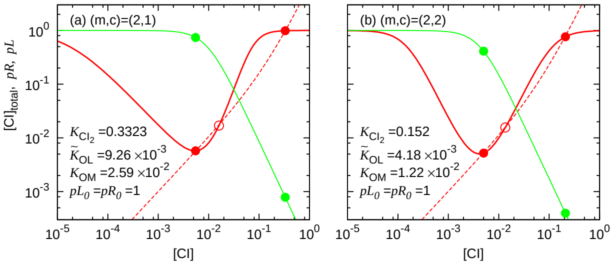

Figure 4: Model A with (a) two MOR monomers and one CI monomer binding to O_M, $(m,c) = (2,1)$, and (b) two MOR monomers and two CI monomers, $(m,c) = (2,2)$. Promoter activities, pL and pR, and $[\mathrm{CI}]_{\mathrm{total}}$ as function of free [CI]. Curves are P_L activity of Eq.(9) (green line), P_R activity of Eq.(25) (solid red line), and $[\mathrm{CI}]_{\mathrm{total}}$ of Eq.(15)(dashed red line). The filled red circles at the intersections represent the stable steady state, and the green circles indicate the P_L activity in the steady states. The open red circles mark the unstable steady states. The repression folds $pR(\mathrm{open})/pR(\mathrm{closed})$ and $pL(\mathrm{open})/pL(\mathrm{closed})$ are approximately 200 and 1000 respectively.

The promoter activities in the two stable states can be determined from the graphic representation in Fig.4. The P_R activity is read from the ordinates of the intersection (filled red circles) and the P_L activity is read off from the corresponding [CI] values of the intersection points (green circles), which allows us to estimate the repression folds for P_L and P_R between the two stable states. The state at the right represents the immune state with open P_R and repressed P_L, while the one at the left represents the anti-immune state with open P_L and repressed P_R .

The relative activities between the two states should be compared with the promoter activities obtained from the *in vivo* measurements [9]; P_L is repressed approximately 1,000-fold in the immune state and P_R approximately 100-fold in the anti-immune state. To reproduce these repression folds in Model A with $(m,c) =$ (2,1) and (2,2), we test the three parameters, K_{CI_2}, $\tilde{K}_{\mathrm{OL}}$, and K_{OM}, representing the dimerization constant of CI,

---

[1] Note that this simplified analysis is based on the assumption that Eq.(5) always holds, i.e. the response of P_L is much faster than that of P_R. For general case, see supplementary material.

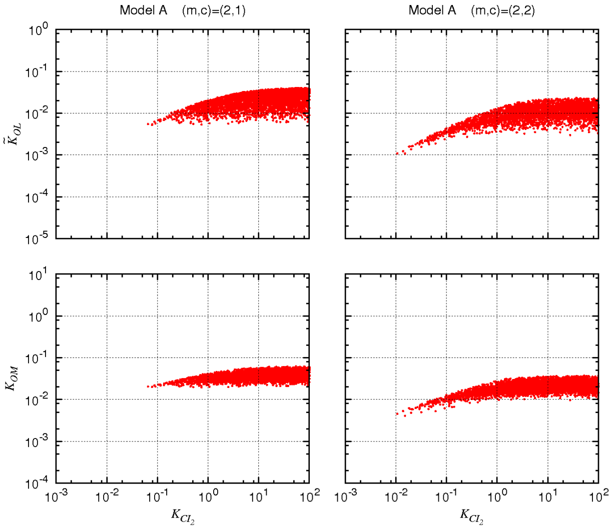

Figure 5: Distributions of possible parameters for Model A. The plotted parameter sets are those that give the repression folds $50 < pR(\text{open})/pR(\text{closed}) < 200$ and $pL(\text{open})/pL(\text{closed}) > 500$ out of 10^6 tested parameter sets, which are randomly picked in the logarithmic scale over the range of $\tilde{K}_{\text{OL}} \in (10^{-5}, 10^{-2})$, $K_{\text{OM}} \in (10^{-4}, 10)$, and $K_{\text{CI}_2} \in (10^{-3}, 10^{2})$.

the effective binding constant of CI-monomer at O_L, and the binding constant of the MOR:CI complex at O_M, respectively, by setting *the criterion that the P_R repression fold should be in the range from 50 to 200 (* $50 < pR(\text{open})/pR(\text{closed}) < 200$*) and the P_L repression fold should at least be 500 (*$pL(\text{open})/pL(\text{closed}) > 500$*).* Fig.5 shows the distributions of accepted values of parameters out of randomly chosen values in the logarithmic scale. $\tilde{K}_{\text{OL}}$ and K_{OM} are narrowly distributed while K_{CI_2} are larger than 10^{-1} for $(m, c) = (2, 1)$ and larger than 10^{-2} for (2,2) in the unit of CI concentration at full activity of P_R. One can also see that the accepted values for K_{CI_2} are much larger than $\tilde{K}_{\text{OL}}$. This suggests that, in order for Model A to work, CI must exist as a monomer and act by cooperative binding to form CI_2 at O_L when repressing P_L.

Figure 6 shows the parameters that satisfy the criterion only for the P_R repression fold versus resulting P_L repression fold (left two columns for Model A and right two for Model B). The vertical green lines are drawn at the P_L repression fold 500, thus only the plots on the right side of the lines should be accepted by the repression fold criterion. From the plots for K_{CI_2} for Model A, one can see that the relatively high values for K_{CI_2} in this model comes from the requirement for the large P_L repression fold. This can be understood as follows; In order to achieve large repression fold for P_L, the difference in [CI] for the two steady states should be large, which in turn requires smaller slope in the $[\text{CI}]_{\text{total}}$ curve, namely larger K_{CI_2} because the slope in $[\text{CI}]_{\text{total}}$ changes from 1 to 2 around $[\text{CI}] \approx K_{\text{CI}_2}$ (Fig.4).

Model B

Now, we consider the possibility that P_R is repressed by a MOR:CI complex formed in cytoplasm before binding to DNA. Examples for Model B are shown in Fig.7, where the P_L activity of Eq.(9) (green line), the P_R activity of Eq.(22) (solid red line), and the total density of CI of Eq.(23) (dashed red line) as a function of [CI] in the logarithmic scale; All of them have three steady states.

Striking difference from the case of Model A is that the $[\text{CI}]_{\text{total}}$ (dashed red line) can be non-monotonic. Therefore, for a given $[\text{CI}]_{\text{total}}$ within a certain range, there exist three possible states with different [CI]. This suggests that the bistability could be obtained for the system with P_L even if P_R were not regulated, namely, even if P_R would produce CI at a fixed rate within the range. This bistability is due to the MOR:CI heteromer formation in cytoplasm; P_L produces MOR, which sequesters its own repressor, i.e. CI, by forming MOR:CI. For a given $[\text{CI}]_{\text{total}}$, the state at low [CI] is the state where most of CI's are incorporated in MOR:CI heterodimers due to the MOR produced by P_L, while the state at high [CI] is the state where most of CI is in the dimer with P_L being repressed. The state in the middle is unstable. Such bistability is, of course, not the bistability observed in the experiments, but one can see that this feature of behavior in $[\text{CI}]_{\text{total}}$ (dashed red line) makes it easier to have three intersections with the P_R activity curve (solid red line) than in the case of Model A.

According to the stability criterion we discussed, the steady state at both ends are stable while the state in the middle is unstable even for the system where both P_R and P_L are regulated. Full analysis, however, shows there are some cases where the states at both ends can be unstable although the stability criterion is correct for most cases (See supplementary material). We analyse the bistability based upon the stability criterion, ignoring the small possibility that the states at both ends could be unstable.

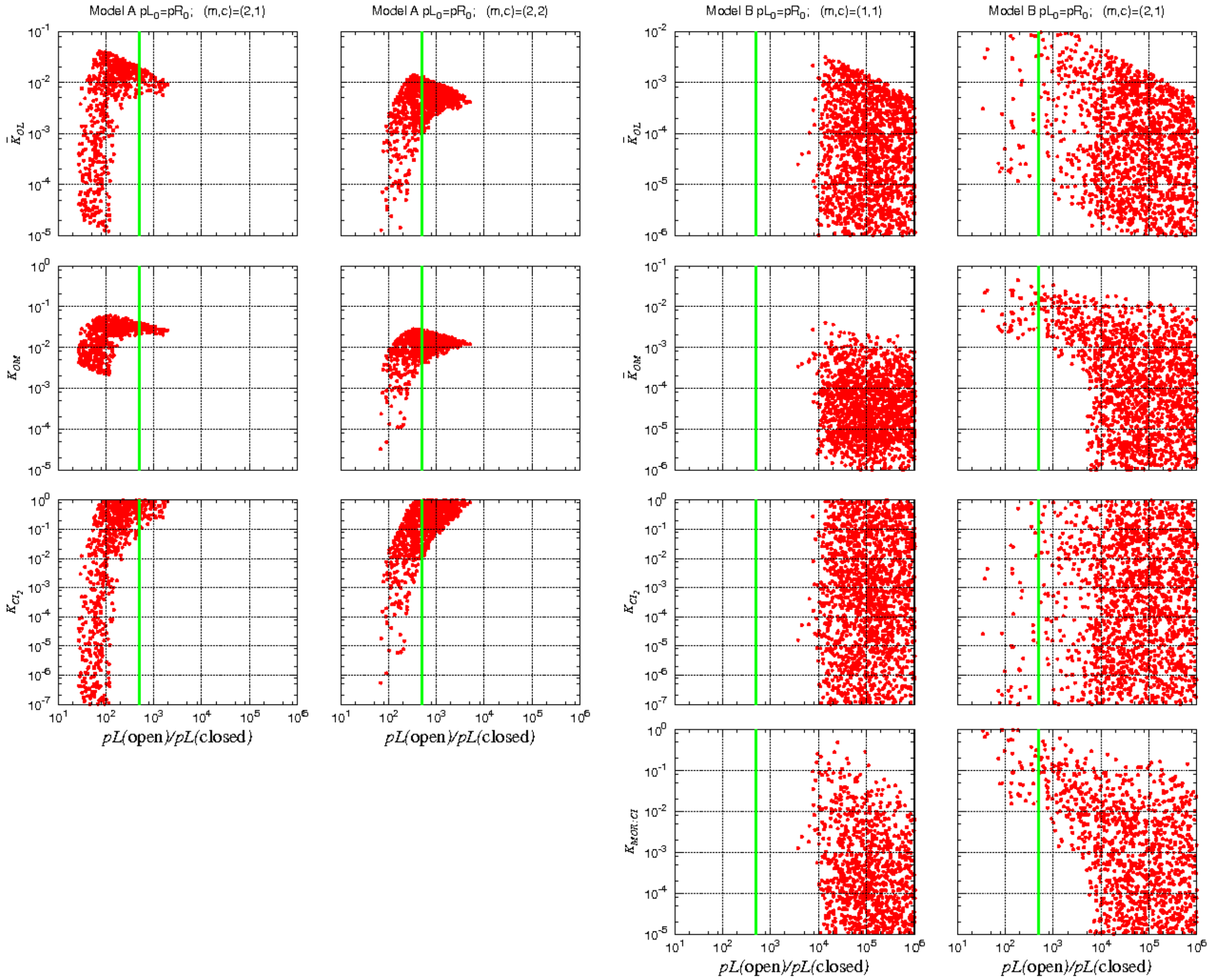

Figure 6: Distribution of possible parameters versus PL repression fold, $pL(\text{open})/pL(\text{closed})$ for Model A with (m, c)=(2,1) and (2,2), and for Model B with (m, c)=(1,1) and (2,1). The plotted parameters are those that satisfy the PR repression fold criterion $50 < pR(\text{open})/pR(\text{closed}) < 200$ out of randomly chosen parameters from the region $\tilde{K}_{\rm OL}, K_{\rm OM}, K_{\rm CI_2} \in [10^{-7}, 1]$ for Model A and $\tilde{K}_{\rm OL}, \tilde{K}_{\rm OM}, K_{\rm CI_2}, K_{\rm MOR:CI} \in [10^{-7}, 1]$ for Model B. Vertical green lines are drawn at PL repression fold 500, thus only the parameters that are in the right side of the lines are consistent with the experimentally obtained repression folds. The number of tested data are 10^6 for Model A with $(m, c) = (2, 1)$, 5×10^6 for Model A with $(m, c) = (2, 2)$, and 2×10^5 for Model B. Note that the effective affinity $\tilde{K}_{\rm OM}$ for Model B is defined by $\tilde{K}_{\rm OM}^{m+c} \equiv K_{\rm OM} K_{\rm MOR_m CI_c}^{m+c-1}$.

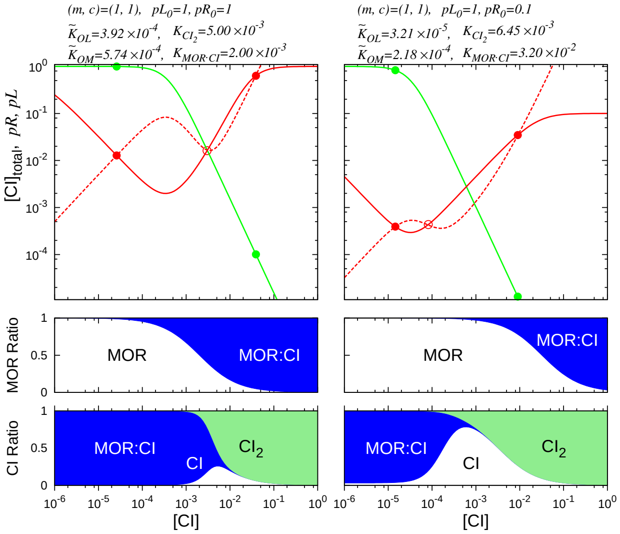

Figure 7: Model B with MOR CI binding to O_M, $(m, c) = (1, 1)$. The bare promoter activities, pL_0 and pR_0, are equal in left panel while the bare activity pL_0 is 10 times stronger than pR_0 in the right panel. The upper graphs show examples of the promoter activities, pL and pR, and $[CI]_{total}$ as a function of [CI]. The repression folds of P_L and P_R are approximately 1000 and 50, respectively in the left figure, and approximately 60,000 and 100 in the right figure. The middle graphs show the ratios of MOR units in the forms of monomer and heteromer, and the lower graphs show the ratios of CI units in the form of monomer, dimer, and heteromer. One can see that MOR:CI and CI_2 compete for the free CI units in the intermediate concentration range of [CI].

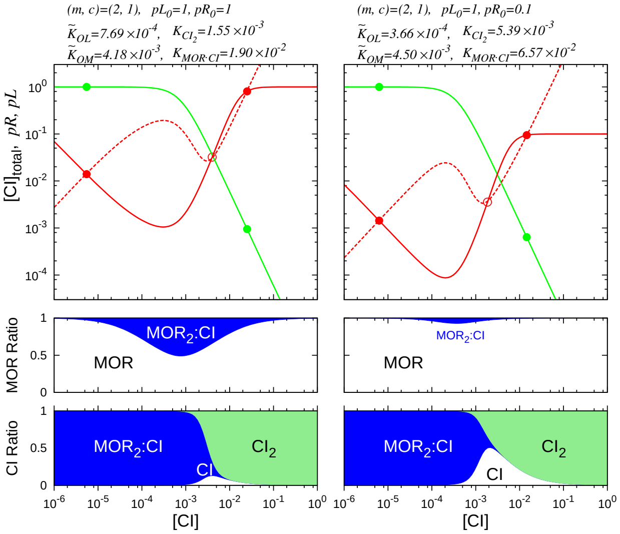

Figure 8: Model B with MOR_2CI binding to O_M, $(m, c) = (2, 1)$. The bare promoter activities, pL_0 and pR_0, are equal in left panel while the bare activity pL_0 is 10 times stronger than pR_0 in the right panel. The upper graphs show examples of the promoter activities, pL and pR, and $[CI]_{total}$ as a function of [CI]. The repression folds of P_L and P_R are approximately 1,000 and 50, respectively, in left figure, and approximately 1,000 and 60 in right figure. In contrast to the case with $(m, c) = (1, 1)$ in Fig.7, the heteromer MOR_2:CI is not formed at high [CI] because the P_L promoter is closed faster than the MOR_2:CI is formed. Note that the effective affinity of O_M is $\tilde{K}_{OM} = (K_{OM} K^2_{MOR\cdot CI})^{1/3}$.

We also examine Model B in the case where a larger complex, MOR_mCI_c, represses P_R. Detailed formalism is given in the appendix.

Figure 8 shows the plots for the extended Model B with $(m, c) = (2, 1)$. This version of the model shows sharper transition between the MOR_2CI regime and the CI_2 regime for the form of CI protein as one can see in the lower graphs for CI ratio. As for the form of MOR, substantial fraction of MOR_2CI appears only in the intermediate range of [CI] in contrast to the case of the MOR CI heterodimer in Fig.7. This is because there are not enough MOR's in the high [CI] region to form MOR_2CI complex because it requires two MOR proteins.

In the right two columns of Fig.6, the parameters that give the P_R repression fold in the range [50, 200] are plotted versus the resulting P_L repression fold for Model B. The 2×10^5 parameter sets are chosen randomly over the range of $[10^{-7}, 1]$ for $\tilde{K}_{OL}$, $\tilde{K}_{OM}$, K_{CI_2}, and $K_{MOR:CI}$. One can see that broad range of parameter sets satisfy the repression fold criterion for P_R, but the resulting repression folds for P_L are limited to the region larger than 5,000 for $(m, c) = (1, 1)$ and 50 for (2,1).

3. Discussion

3.1. Summary

The bacteriophage TP901-1 has provided us with a conceptually new design of a genetic switch, in which the interaction between two antagonistic regulators, CI and MOR, is essential. Bistability between the immune and the ant-immune states has been demonstrated with a genetic switch that consists of the two divergently oriented promoters P_L and P_R, the two promoter-proximal genes, *cI* and *mor*, and only one of the three CI operator sites O_L on a low copy number plasmid [8, 9]. The repression folds in the two states have been determined by *in vivo* measurements as around 1,000-fold for P_L repression in the immune state and around 100-fold for P_R repression in the anti-immune state.

We constructed mathematical models for this cloned bistable system, assuming a putative operator O_M to regulate P_R (Fig.1b). We assumed that P_L is repressed by CI_2 bound to O_L whereas P_R is repressed by the MOR_mCI_c:DNA complex on O_M . We examined two types of models: one where MOR and CI interact only on DNA (Model A), and the other where MOR and CI form MOR_mCI_c complex in cytoplasm first and then the

Parameter Ranges for Model A		
(m, c)	(2,1)	(2,2)
$\tilde{K}_{\mathrm{OL}}$	$\sim 10^{-2}$	$10^{-3} \sim 10^{-2}$
K_{OM}	$10^{-2} \sim 10^{-1}$	$\sim 10^{-3}$
$K_{\mathrm{CI_2}}$	$\gtrsim 10^{-2}$	$\gtrsim 10^{-2}$

Table 1: Accepted ranges of parameters for Model A. The values are given in the unit of the concentrations that correspond to [CI] and [MOR] at the full activity of the promoter $\mathrm{P_R}$ and $\mathrm{P_L}$, respectively.

Parameter Ranges for Model B		
(m, c)	(1,1)	(2,1)
$\tilde{K}_{\mathrm{OL}}$	$\lesssim 3 \times 10^{-3}$	$(3 \times 10^{-6}) \sim 3 \times 10^{-2}$
$\tilde{K}_{\mathrm{OM}}$	$\lesssim 5 \times 10^{-3}$	$(10^{-4}) \sim 3 \times 10^{-2}$
$K_{\mathrm{CI_2}}$	—	—
$K_{\mathrm{MOR:CI}}$	$\lesssim 3 \times 10^{-1}$	$(10^{-3}) \sim 1$

Table 2: Accepted ranges of parameters for Model B. The values are given in the unit of the concentrations that correspond to [CI] and [MOR] at the full activity of the promoter $\mathrm{P_R}$ and $\mathrm{P_L}$, respectively. The values in the parentheses are the lower limits when the fold criterion for $\mathrm{P_L}$ is restricted to $500 < pL(\mathrm{open})/pL(\mathrm{closed}) < 5000$. The ranges for $K_{\mathrm{CI_2}}$ cannot be set because the accepted values extends over the whole tested range.

complex binds to $\mathrm{O_M}$ (Model B). For each model, we tested bistability and performed parameter scans using the criterion that the repression folds should be consistent with the experiments.

Our results are summarized as follows: For Model A, (i) the system shows bistability only when $2m - c \geq 2$, (ii) the possible values for the operator affinities $\tilde{K}_{\mathrm{OL}}$ and K_{OM} are narrowly distributed, (iii) the possible dissociation constant $K_{\mathrm{CI_2}}$ is much larger than the operator affinity $\tilde{K}_{\mathrm{OL}}$ due to the large repression fold for $\mathrm{P_L}$, (iv) the possible value for $K_{\mathrm{CI_2}}$ is bounded by the relatively large lower limit. The accepted ranges for the parameters are listed in Table 1. For Model B, (i) the bistability is robust due to the sequestration of CI by the $\mathrm{MOR}_m\mathrm{CI}_c$ complex formation, (ii) large parameter regions are allowed by the repression fold criterion, (iii) the $\mathrm{P_L}$ repression fold is bounded by the lower limit for the parameters that are consistent with the $\mathrm{P_R}$ repression fold: $pL(\mathrm{open})/pL(\mathrm{closed}) > 5000$ for $(m, c) = (2, 1)$, and > 50 for $(m, c) = (2, 2)$. The accepted ranges for the parameters are listed in Table 2.

3.2. Validity of the Models

In order to assess validity of the models, we have to determine our unit for CI concentration first. We employed the unit where [CI] is measured by the concentration in the steady state with the full activity of $\mathrm{P_L}$. This concentration should be compared with [CI] in the immune state of *in vivo* experiment on the system with around 10 copy-number plasmid containing the modified switch. We estimate this as follows by using the value of 300 nM for the CI concentration in the lysogenic/immune state of the wild lambda phage [20]; First, we assume that this concentration is comparable with that for wild type TP901-1 with a single copy. Then, we multiply this by the following two factors: the factor 10 of the copy-number of plasmid, and the factor 100 of the relative activity of $\mathrm{P_R}$ in our modified system in comparison with the wild type switch [9]. With these factors, we estimate that pR_0, i.e., [CI] at the full $\mathrm{P_R}$ activity in the present system, could be well over 10^5 nM scale.

Model A. With this unit, we might be able to rule out Model A based upon the estimated values of $\tilde{K}_{\mathrm{OL}}$ and $K_{\mathrm{CI_2}}$. The possible value of $\tilde{K}_{\mathrm{OL}}$ in Model A is between around 10^{-3} and 5×10^{-2} (Table 1), but this contradicts the *in vitro* estimate of 28 nM for the CI concentration at which $\mathrm{O_L}$ is occupied by CI for 50% of the time[10]. The lower limit of $\tilde{K}_{\mathrm{OL}} \sim 10^{-3}$ in Model A should correspond to 100 nM or quite possibly even larger, but it is already well above 28 nM, i.e., the *in vivo* estimate for repressor-DNA affinity for TP901-1.

We also found that the large repression fold of $\mathrm{P_L}$ entails $K_{\mathrm{CI_2}} \gg \tilde{K}_{\mathrm{OL}}$ for Model A. This means that CI's exist as monomers in cytoplasm and form $\mathrm{CI_2}$ when they bind to $\mathrm{O_L}$, but this is in contrast with many phage-encoded repressor proteins, such as those encoded by phage lambda, 434, and 186, which tend to exist as dimers or higher oligomers in solution[21, 22, 23, 24]; Actually, most of the 434 and lambda repressors exist in the dimeric conformation at nanomolar concentrations [23, 21]. Our Model A challenges the presumption that the formation of dimers is a prerequisite for its specific DNA binding.

Model B. We found broader distribution of parameter sets that satisfy the repression fold criterion for Model B. In particular, we did not find lower bounds for possible $K_{\mathrm{CI_2}}$ in contrast to the case of Model A.

In the comparison of the two variants of Model B, our results show that the model with the formation of $\mathrm{MOR_2CI}$ complex is more favorable than that with

MOR CI. For the model with MOR CI, the PL repression fold turned out to be always larger than 5,000 for the parameters that give the PR repression fold between 50 through 200. Such a high repression fold of PL has never been actually observed *in vivo*. On the other hand, for the model with MOR_2CI, the lower bound for the resulting PL repression fold can be as low as 50, which covers the observed range of the PL repression fold. As for the parameter ranges, this variant of Model B gives $\tilde{K}_{\rm OM} \gtrsim 0.2 \times 10^{-4}$ and $K_{\rm MOR:CI} \gtrsim 10^{-3}$ when the repression fold for PL is smaller than 5,000 (Fig.6).

3.3. *Experimental Test*

One of the distinguishing consequences of Model B is that the system with uncontrolled PR can be bistable because of the sequestration of CI by MOR:CI complex formation. Even if PR produces CI at a constant rate, there can be the two stable states: one with the repressed PL and the other with the derepressed PL. Such a mechanism of bistability has been proposed by François and Hakim [12, 13] as a theoretical possibility. Our study suggests this mechanism is employed in TP901-1. This may be tested experimentally for the genetic switch of phage TP901-1 by measuring the promoter activity of PL in systems containing a functional *mor* gene and expressing CI from uncontrolled PR promoters at constant but various rates. Plotting the PL activity of each system versus the uncontrolled PR activity, one should find a characteristic feature for bistability as in Fig.9, where the PL activity is doubled-valued for a certain range of the PR activity.

3.4. *Concluding Remark*

The genetic switching mechanism in TP901-1 is remarkably robust; The modified system studied here with only one operator OL contains 100 times more CI molecules in its immune state than the wild type genetic switch with all of the three operators on plasmids, yet still shows bistability. Our model study suggests that the robustness of the genetic switch in TP901-1 is brought about by sequestration of CI through MOR:CI complex formation in cytoplasm.

Acknowledgements

This work was supported by the Danish National Research Foundation through the Center for Models of Life.

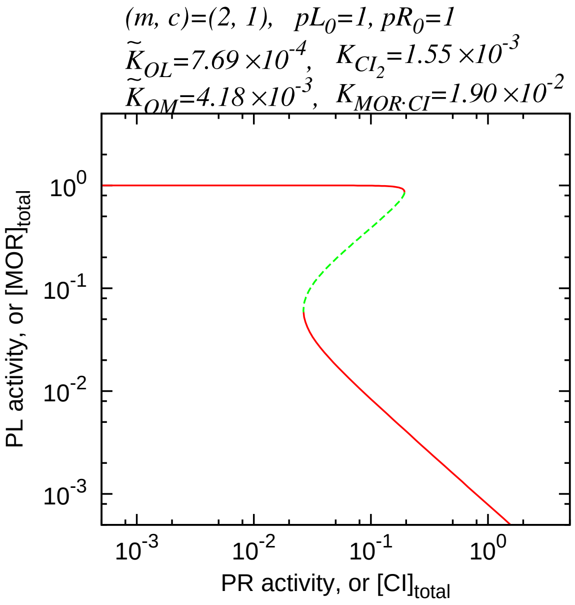

Figure 9: The PL activity (or $[\mathrm{MOR}]_{\rm total}$) versus the PR activity (or $[\mathrm{CI}]_{\rm total}$) for the system with uncontrolled PR. The solid lines show the stable states and the dashed line shows the unstable state.

Appendix: Formalism for Model B with $(m, c) = (2, 1)$

In the appendix, we present some of the formulae we used for Model B with $(m, c) = (2, 1)$. For this case, the promoter PR activity is a function of MOR_2CI concentration,

$$pR([\mathrm{MOR}], [\mathrm{CI}]) = pR_0 \frac{1}{1 + [\mathrm{MOR_2CI}]/K_{\rm OM}}, \tag{26}$$

and $[\mathrm{MOR_2CI}]$ is given by

$$[\mathrm{MOR_2CI}] = \frac{[\mathrm{MOR}]^2 \cdot [\mathrm{CI}]}{K^2_{\rm MOR:CI}}, \tag{27}$$

with the dissociation constant $K_{\rm MOR:CI}$.

The total concentrations of CI and MOR are now

$$\begin{aligned} [\mathrm{CI}]_{\rm total} &= [\mathrm{CI}] + 2[\mathrm{CI_2}] + [\mathrm{MOR_2CI}], && (28) \\ [\mathrm{MOR}]_{\rm total} &= [\mathrm{MOR}] + 2[\mathrm{MOR_2CI}], && (29) \end{aligned}$$

thus the corresponding equations with Eq.(20) in the main text becomes

$$[\mathrm{MOR}] = \frac{K^2_{\rm MOR:CI}}{4[\mathrm{CI}]} \left(-1 + \sqrt{1 + 8[\mathrm{CI}][\mathrm{MOR}]_{\rm total}/K^2_{\rm MOR:CI}} \right). \tag{30}$$

Thus, both sides of the steady state condition Eq.(6) are now given by

$$pR([\mathrm{MOR}], [\mathrm{CI}]) = pR_0 \frac{1}{1 + [\mathrm{MOR}]^2[\mathrm{CI}]/\tilde{K}_{\mathrm{OM}}^3} \quad (31)$$

$$[\mathrm{CI}]_{\mathrm{total}} = [\mathrm{CI}] + 2\frac{[\mathrm{CI}]^2}{K_{\mathrm{CI}_2}} + \frac{1}{2}\Big([\mathrm{MOR}]_{\mathrm{total}} - [\mathrm{MOR}]\Big) \quad (32)$$

with [MOR] by Eq.(30) and $[\mathrm{MOR}]_{\mathrm{total}}$ by Eq.(5). The effective affinity $\tilde{K}_{\mathrm{OM}}$ is defined as

$$\tilde{K}_{\mathrm{OM}} \equiv (K_{\mathrm{OM}} K_{\mathrm{MOR:CI}}^2)^{1/3}. \quad (33)$$

References

[1] D. Dubnau, R. Losick, Bistability in bacteria, Mol. Microbiol. 61 (2006) 564–572.

[2] J. Veening, W. Smits, O. Kuipers, Bistability, Epigenetics, and Bet-Hedging in Bacteria, Annu. Rev. Microbiol. 62 (2008) 193–210.

[3] J. Rerrell, Self-perpetuating states in signal transduction: positive feedback, double-negative feedback and bistability, Current Opinion in Cell Biology 14 (2002) 140–148.

[4] H. Eisen, P. Brachet, L. P. da Silva, F. Jacob, Regulation of Repressor Expression in λ, Proc. Natl. Acad. Sci. USA 66 (1970) 855–862.

[5] S. L. Svenningsen, N. Costantino, D. L. Court, S. Adhya, On the role of Cro in λ prophage induction, Proc. Natl. Acad. Sci. USA 102 (2005) 4465–4469.

[6] M. Ptashne, A Genetic Switch, third edition Edition, Cold Spring Harbor Laboratory Press, New York, 2004.

[7] M. Pedersen, L. Leggio, J. Grossmann, S. Larsen, K. Hammer, Identification of Quaternary Structure and Functional Domains of the CI Repressor from Bacteriophage TP901-1, J. Mol. Biol. 376 (2008) 983–996.

[8] P. Madsen, A. Johansen, K. Hammer, L. Brondsted, The Genetic Switch Regulating Activity of Early Promoters of the Temperate Lactococcal Bacteriophage TP901-1, J. Bacteriol. 181 (1999) 7430–7438.

[9] M. Pedersen, K. Hammer, The role of MOR and the CI operator sites on the genetic switch of the temperate bacteriophage TP901-1, J. Mol. Biol. 384 (2008) 577–589.

[10] A. Johansen, L. Brondsted, K. Hammer, Identification of operator sites of the CI repressor of phage TP901-1: evolutionary link to other phages, Virology 311 (2003) 144–156.

[11] L. J. W. Shimon, S. C. Harrison, The Phage 434 OR2/R1-69 Complex at 2.5Å Resolution, J. Mol. Biol. 232 (1993) 826–838.

[12] P. François, V. Hakim, Design of genetic networks with specified functions by evolution in silico, Proc. Natl. Acad. Sci. USA 101 (2004) 580–585.

[13] P. François, V. Hakim, Core genetic module: The mixed feedback loop, Phys. Rev. E 72 (2005) 031908–1–14.

[14] N. E. Buchler, M. Louis, Molecular Titration and Ultrasensitivity in Regulatory Networks, J. Mol. Biol. 384 (2008) 1106–1119.

[15] N. E. Buchler, F. R. Cross, Protein sequestration generates a flexible ultrasensitive reponse in a genetic network, Mol. System Biol. 5 (2009) 272–1–7.

[16] H. Nakanishi, N. Mitarai, K. Sneppen, Dynamical Analysis on Gene Activity in the Presence of Repressors and an Interfering Promoter, Biophysical J. 95 (2008) 4228–4240.

[17] G. K. Ackers, A. D. Johnson, M. A. Shea, Quantitative model for gene regulation by lambda phage repressor, Proc. Natl. Acad. Sci. USA 79 (1982) 1129–1133.

[18] K. Sneppen, I. B. Dodd, K. E. Shearwin, A. C. Palmer, R. A. Schubert, B. P. Callen, J. B. Egan, A mathematical model for transcriptional interference by RNA polymerase traffic in Escherichia coli, J. Mol. Biol. 346 (2005) 399–409.

[19] I. B. Dodd, K. E. Shearwin, K. Sneppen, Modeling transcriptional interference and DNA looping in gene regulation, J. Mol. Biol. 369 (2007) 1200–1213.

[20] L. Reichardt, A. D. Kaiser, Control of λ Repressor Synthesis, Proc. Natl. Acad. Sci. USA 68 (1971) 2185–2189.

[21] K. S. Koblan, G. K. Ackers, Energetics of Subunit Dimerization in Bacteriophage λ *c*I Repressor: Linkage to Protons, Temperature, and KCl, Biochemistry 30 (1991) 7817–7821.

[22] M. Ciubotaru, F. Bright, C. Ingersoll, G. Koudelka, DNA-induced conformational changes in bacteriophage 434 repressor, J. Mol. Biol. 294 (1999) 859–873.

[23] P. Neufing, K. Shearwin, J. Egan, Establishing lysogenic transcription in the temperate coliphage 186, J. Bacteriol. 183 (2001) 2376–2379.

[24] K. E. Shearwin, I. B. Dodd, J. B. Egan, The Helix-Turn-Helix Motif of the Coliphage 186 Immunity Repressor Binds to Two Distinct Recognition Sequences, J. Biol. Chem. 277 (2002) 3186–3194.

Supplementary material for
“Model Analysis of the Genetic Switch Isolated from the Temperate Bacteriophage TP901-1:
Repressor Sequestration Effect”

Hiizu Nakanishi[a], **Margit Pedersen**[b], **Anne K. Alsing**[b], **and Kim Sneppen**[b]

[a]*Department of Physics, Kyushu University 33, Fukuoka 812-8581, Japan*
[b]*Niels Bohr Institute, Copenhagen University, Denmark*

The stability criterion for the steady state used in the manuscript is examined. Dynamical analysis shows that the criterion is valid as long as the $[\mathrm{CI}]_{\mathrm{total}}$ curve is a monotonically increasing function. In Model B, however, the $[\mathrm{CI}]_{\mathrm{total}}$ curve has a part with negative slope for some parameter region, in which case the stability cannot be determined only by comparing the slopes of the curves. The steady state at the left side could be unstable when it is loacated in the region where $[\mathrm{CI}]_{\mathrm{total}}$ is decreasing.

1. Steady States

The steady states satisfy the self-consistent conditions

$$pL\big([CI]\big) = [MOR]_{\mathrm{tot}}\big([MOR],[CI]\big) \tag{1}$$

$$pR\big([MOR],[CI]\big) = [CI]_{\mathrm{tot}}\big([CI],[MOR]\big), \tag{2}$$

with

$$[CI]_{\mathrm{tot}}\big([CI],[MOR]\big) = [CI] + 2[CI_2] + [MOR\cdot CI] \tag{3}$$

$$[MOR]_{\mathrm{tot}}\big([MOR],[CI]\big) = [MOR] + [MOR\cdot CI]. \tag{4}$$

Here, $[CI_2]$, $[MOR\cdot CI]$ are equilibrium concentrations of the protein complexes.

We determined the steady solutions graphically by looking for intersections of the following two curves as a function of $[CI]$, i.e. the production curve and the $[\mathrm{CI}]_{\mathrm{total}}$ curve that represents degradation rate:

$$pR = pR\Big([MOR],\ [CI]\Big) \tag{5}$$

$$[CI]_{\mathrm{tot}} = [CI]_{\mathrm{tot}}\Big([CI],[MOR]\Big), \tag{6}$$

with $[MOR]$ being a function of $[MOR]_{\mathrm{tot}}$ and $[CI]$ derived from the relation $[MOR]_{\mathrm{tot}}([MOR],[CI])$, and $[MOR]_{\mathrm{tot}}$ being given by $pL([CI])$,

$$[MOR] = [MOR]\big([MOR]_{\mathrm{tot}},\ [CI]\big) = [MOR]\big(pL([CI]),\ [CI]\big). \tag{7}$$

2. Stability criterion

In the text, the stability of the steady state is determined by the simple criterion. Let the slope of the production curve and the degradation curve be denoted by

$$\frac{\mathrm{d}\, pR}{\mathrm{d}[CI]} \quad \text{and} \quad \frac{\mathrm{d}\, [CI]_{\mathrm{tot}}}{\mathrm{d}[CI]},$$

respectively. Then the criterion is

$$\begin{array}{rl} \text{the steady state is stable} & \text{if } \dfrac{\mathrm{d}\, pR}{\mathrm{d}[CI]} < \dfrac{\mathrm{d}\, [CI]_{\mathrm{tot}}}{\mathrm{d}[CI]}, \\[2ex] \text{the steady state is unstable} & \text{if } \dfrac{\mathrm{d}\, pR}{\mathrm{d}[CI]} > \dfrac{\mathrm{d}\, [CI]_{\mathrm{tot}}}{\mathrm{d}[CI]} \end{array} \tag{8}$$

at the corresponding intersection.

This criterion is simple and plausible, but based on the single variable picture although the system has at least two dynamical variables: $[CI]$ and $[MOR]$. The full analysis for stability requires dynamical consideration.

3. Dynamical Analysis of Stability

The dynamics for the protein concentrations is given by the set of equations:

$$\frac{d}{dt}[MOR]_{\mathrm{tot}} = \frac{1}{\tau_M}\Big(pL([CI]) - [MOR]_{\mathrm{tot}}\Big) \tag{9}$$

$$\frac{d}{dt}[CI]_{\mathrm{tot}} = \frac{1}{\tau_C}\Big(pR([MOR],[CI]) - [CI]_{\mathrm{tot}}\Big). \tag{10}$$

The total concentrations $[CI]_{\mathrm{tot}}$ and $[MOR]_{\mathrm{tot}}$ are given by eqs.(3) and (4). Basic assumption for this is that the equilibration among protein complexes in cytoplasm is much faster than the decay rates of CI and MOR: $1/\tau_C$ and $1/\tau_M$.

Consider the steady solution with $[CI]^*$ and $[MOR]^*$, which satisfies eqs.(1) and (2). Suppose the steady state is perturbed by small fluctuation as

$$[CI] = [CI]^* + \delta[CI] \tag{11}$$

$$[MOR] = [MOR]^* + \delta[MOR], \tag{12}$$

and see if the small deviation will grow or decay in time.

By inserting these into eqs.(9) and (10), we obtain the equations for the time evolution of $\delta[CI]$ and $\delta[MOR]$,

$$\begin{pmatrix} \left(\dfrac{\partial M_t}{\partial C}\right)^*, & \left(\dfrac{\partial M_t}{\partial M}\right)^* \\[2ex] \left(\dfrac{\partial C_t}{\partial C}\right)^*, & \left(\dfrac{\partial C_t}{\partial M}\right)^* \end{pmatrix} \begin{pmatrix} \delta\dot{C} \\[2ex] \delta\dot{M} \end{pmatrix} =$$

$$\begin{pmatrix} \frac{1}{\tau_M}\left\{\left(\frac{\partial L}{\partial C}\right)^* - \left(\frac{\partial M_t}{\partial C}\right)^*\right\}, & -\frac{1}{\tau_M}\left(\frac{\partial M_t}{\partial M}\right)^* \\ \frac{1}{\tau_C}\left\{\left(\frac{\partial R}{\partial C}\right)^* - \left(\frac{\partial C_t}{\partial C}\right)^*\right\}, & \frac{1}{\tau_C}\left\{\left(\frac{\partial R}{\partial M}\right)^* - \left(\frac{\partial C_t}{\partial M}\right)^*\right\} \end{pmatrix}\begin{pmatrix}\delta C \\ \delta M\end{pmatrix}, \tag{13}$$

where we employ the abbreviated notations:

$$M_t \equiv [MOR]_{\mathrm{tot}}, \quad M \equiv [MOR], \quad C_t \equiv [CI]_{\mathrm{tot}}, \quad C \equiv [CI], \quad L \equiv pL, \quad R \equiv pR.$$

We further abbreviate the notation as

$$M_{t,C} \equiv \left(\frac{\partial M_t}{\partial C}\right)^* = \left(\frac{\partial [MOR]_{\mathrm{tot}}}{\partial [CI]}\right)^*, \quad L_{,C} \equiv \left(\frac{\partial L}{\partial C}\right)^* = \left(\frac{\partial\, pL([CI])}{\partial [CI]}\right)^*, \quad \text{etc.}$$

then eq.(13) is expressed as

$$\begin{pmatrix} M_{t,C}\,, & M_{t,M} \\ C_{t,C}\,, & C_{t,M} \end{pmatrix}\begin{pmatrix}\delta\dot{C} \\ \delta\dot{M}\end{pmatrix} = \begin{pmatrix} \frac{1}{\tau_M}\left(L_{,C} - M_{t,C}\right), & -\frac{1}{\tau_M}M_{t,M} \\ \frac{1}{\tau_C}\left(R_{,C} - C_{t,C}\right), & \frac{1}{\tau_C}\left(R_{,M} - C_{t,M}\right) \end{pmatrix}\begin{pmatrix}\delta C \\ \delta M\end{pmatrix}. \tag{14}$$

4. The criterion is always valid for Model A:

In the case of Model A, $[MOR \cdot CI] = 0$, thus we have

$$C_{t,M} = 0, \quad M_{t,M} = 1, \quad M_{t,C} = 0,$$

then eq.(14) becomes

$$\begin{pmatrix} 0, & 1 \\ C_{t,C}, & 0 \end{pmatrix}\begin{pmatrix}\delta\dot{C} \\ \delta\dot{M}\end{pmatrix} = \begin{pmatrix} \frac{1}{\tau_M}L_{,C}\,, & -\frac{1}{\tau_M} \\ \frac{1}{\tau_C}\left(R_{,C} - C_{t,C}\right), & \frac{1}{\tau_C}R_{,M} \end{pmatrix}\begin{pmatrix}\delta C \\ \delta M\end{pmatrix}. \tag{15}$$

Now we assume the solution as

$$\delta C, \quad \delta M \propto e^{\omega t}$$

then we have

$$\begin{pmatrix} \frac{1}{\tau_M}L_{,C}, & -\frac{1}{\tau_M} - \omega \\ \frac{1}{\tau_C}\left(R_{,C} - C_{t,C}\right) - C_{t,C}\,\omega, & \frac{1}{\tau_C}R_{,M} \end{pmatrix}\begin{pmatrix}\delta C \\ \delta M\end{pmatrix} = 0. \tag{16}$$

The condition that this equation has non-zero solution gives

$$-\,C_{t,C}\,\omega^2 + \left[\frac{1}{\tau_C}\left(R_{,C} - C_{t,C}\right) - \frac{1}{\tau_M}C_{t,C}\right]\omega + \frac{1}{\tau_M\tau_C}\left[L_{,C}R_{,M} + R_{,C} - C_{t,C}\right] = 0 \tag{17}$$

If all the solutions ω have a negative real part, the state is stable, whereas the state is unstable if there is a solution with a positive real part.

Note that the slopes of the production curve and the degradation curve are given by

$$\frac{\mathrm{d}\,pR}{\mathrm{d}CI} \equiv \left(\frac{\mathrm{d}\,pR([MOR],[CI])}{\mathrm{d}[CI]}\right)^{*} = L_{,C}R_{,M} + R_{,C} \tag{18}$$

$$\frac{\mathrm{d}CI_{\mathrm{tot}}}{\mathrm{d}CI} \equiv \left(\frac{\partial[CI]_{\mathrm{tot}}([CI])}{\partial[CI]}\right)^{*} = C_{t,C}. \tag{19}$$

Using these, eq.(17) becomes

$$-\frac{\mathrm{d}CI_{\mathrm{tot}}}{\mathrm{d}CI}\,\omega^2 + \left[\frac{1}{\tau_C}\left(\frac{\mathrm{d}\,pR}{\mathrm{d}CI} - \frac{\mathrm{d}CI_{\mathrm{tot}}}{\mathrm{d}CI} - L_{,C}R_{,M}\right) - \frac{1}{\tau_M}\frac{\mathrm{d}CI_{\mathrm{tot}}}{\mathrm{d}CI}\right]\omega + \frac{1}{\tau_C\tau_M}\left[\frac{\mathrm{d}\,pR}{\mathrm{d}CI} - \frac{\mathrm{d}CI_{\mathrm{tot}}}{\mathrm{d}CI}\right] = 0 \tag{20}$$

Note that

$$L_{,C},\quad R_{,C},\quad R_{,M} < 0.$$

(1) The case of $\tau_M \ll \tau_C$. One solution is of order $1/\tau_M$ and the other is of order $1/\tau_C$.

$$\omega \approx \begin{cases} -\dfrac{1}{\tau_M} \\[2ex] \dfrac{1}{\tau_C}\left[\dfrac{\mathrm{d}CI_{\mathrm{tot}}}{\mathrm{d}CI}\right]^{-1}\left[\dfrac{\mathrm{d}\,pR}{\mathrm{d}CI} - \dfrac{\mathrm{d}CI_{\mathrm{tot}}}{\mathrm{d}CI}\right] \end{cases}.$$

This shows the criterion (8) is valid.

(2) The case of $\tau_C \ll \tau_M$. One solution is of order $1/\tau_M$ and the other is of order $1/\tau_C$.

$$\omega \approx \begin{cases} \dfrac{1}{\tau_C}\left[\dfrac{\mathrm{d}CI_{\mathrm{tot}}}{\mathrm{d}CI}\right]^{-1}\left[\dfrac{\mathrm{d}\,pR}{\mathrm{d}CI} - \dfrac{\mathrm{d}CI_{\mathrm{tot}}}{\mathrm{d}CI} - L_{,C}R_{,M}\right] \\[2ex] -\dfrac{1}{\tau_M}\left[\dfrac{\mathrm{d}\,pR}{\mathrm{d}CI} - \dfrac{\mathrm{d}CI_{\mathrm{tot}}}{\mathrm{d}CI} - L_{,C}R_{,M}\right]^{-1}\left[\dfrac{\mathrm{d}\,pR}{\mathrm{d}CI} - \dfrac{\mathrm{d}CI_{\mathrm{tot}}}{\mathrm{d}CI}\right] \end{cases}.$$

The criterion (8) is also valid because

$$\frac{\mathrm{d}CI_{\mathrm{tot}}}{\mathrm{d}CI} > 0,\quad L_{,C}R_{,M} > 0.$$

(3) General case. The criterion (8) can be shown to be valid because eq.(17) always has two real solutions, ω_1 and ω_2, and the sum of the two solutions is negative when the slope of the production curve is less steep than that of the degradation curve, i.e.

$$\omega_1 + \omega_2 < 0 \quad \text{when} \quad \frac{\mathrm{d}\,pR}{\mathrm{d}CI} - \frac{\mathrm{d}CI_{\text{tot}}}{\mathrm{d}CI} < 0.$$

The positivity of the discriminant D of eq.(17):

$$\begin{aligned} D = & \left[\frac{1}{\tau_C}\left\{R_{,C} - C_{t,C}\right\} - \frac{1}{\tau_M} C_{t,C}\right]^2 \\ & \qquad + 4C_{t,C}\frac{1}{\tau_M \tau_C}\left[L_{,C}R_{,M} + R_{,C} - C_{t,C}\right] \\ = & \left[\frac{1}{\tau_C}R_{,C} - \left(\frac{1}{\tau_C} - \frac{1}{\tau_M}\right)C_{t,C}\right]^2 + \frac{4}{\tau_C \tau_M} C_{t,C}R_{,M}L_{,C} > 0, \end{aligned}$$

thus eq.(17) has two real solutions.

5. The criterion is valid for Model B as long as the degradation curve has pisitive slope, but the state may be unstable otherwise.

In this model, the existence of $MOR \cdot CI$ makes the expressions for the slopes of the production curve and the degradation curve a bit more complicated:

$$\begin{aligned} \frac{\mathrm{d}\,pR}{\mathrm{d}CI} \equiv \frac{\mathrm{d}}{\mathrm{d}[CI]}\, & pR\Big([MOR]\big(M_t, [CI]\big),\, [CI]\Big) \\ = & \left(\frac{\partial R}{\partial C}\right)_M + \left(\frac{\partial R}{\partial M}\right)_C \left[\left(\frac{\partial M}{\partial M_t}\right)_C \left(\frac{\partial L}{\partial C}\right) + \left(\frac{\partial M}{\partial C}\right)_{M_t}\right] \\ = & \left(\frac{\partial R}{\partial C}\right)_M + \left(\frac{\partial R}{\partial M}\right)_C \left(\frac{\partial M_t}{\partial M}\right)_C^{-1} \left[\left(\frac{\partial L}{\partial C}\right) - \left(\frac{\partial M_t}{\partial C}\right)_M\right] \\ = & R_{,C} + \frac{R_{,M}}{M_{t,M}}\big(L_{,C} - M_{t,C}\big) \end{aligned} \tag{21}$$

$$\begin{aligned} \frac{\mathrm{d}\,CI_{\text{tot}}}{\mathrm{d}CI} \equiv \frac{\mathrm{d}}{\mathrm{d}[CI]}\, & [CI]_{\text{tot}}\Big([CI], [MOR]\big(M_t,\, [CI]\big)\Big) \\ = & \left(\frac{\partial C_t}{\partial C}\right)_M + \left(\frac{\partial C_t}{\partial M}\right)_C \left[\left(\frac{\partial M}{\partial M_t}\right)_C \left(\frac{\partial L}{\partial C}\right) + \left(\frac{\partial M}{\partial C}\right)_{M_t}\right] \\ = & \left(\frac{\partial C_t}{\partial C}\right)_M + \left(\frac{\partial C_t}{\partial M}\right)_C \left(\frac{\partial M_t}{\partial M}\right)_C^{-1} \left[\left(\frac{\partial L}{\partial C}\right) - \left(\frac{\partial M_t}{\partial C}\right)_M\right] \\ = & C_{t,C} + \frac{C_{t,M}}{M_{t,M}}\big(L_{,C} - M_{t,C}\big), \end{aligned} \tag{22}$$

where the variables that kept constant upon partial differentiation are explicitly indicated as

$$\left(\frac{\partial M}{\partial M_t}\right)_C \equiv \frac{\partial}{\partial [MOR]_{\text{tot}}}[MOR]\Big([MOR]_{\text{tot}}, [CI]\Big)$$

whenever it could be ambiguous. In the derivation, we have used the relations

$$\left(\frac{\partial M}{\partial M_t}\right)_C = \left(\frac{\partial M_t}{\partial M}\right)_C^{-1}, \qquad \left(\frac{\partial M}{\partial C}\right)_{M_t}\left(\frac{\partial M_t}{\partial M}\right)_C\left(\frac{\partial C}{\partial M_t}\right)_M = -1.$$

5.1. Stability of the system with PL with externally controlled $[CI]_{\text{tot}}$

First, we will examine the stability of the system without PR, CI being provided externally. The system is shown to be bistable for some parameter region.

Based upon the approximation that the relaxation in the solution is much faster than the protein production rate by PL, we consider the system where $[CI]$ and $[MOR]$ satisfy

$$\begin{aligned} [CI]_{\text{tot}} &= [CI]_{\text{tot}}\Big([CI], [MOR]\Big) && (23)\\ \frac{d}{dt}[MOR]_{\text{tot}} &= \frac{1}{\tau_M}\Big(pL([CI]) - [MOR]_{\text{tot}}\Big), && (24)\end{aligned}$$

thus the deviation from the steady state follows

$$\begin{aligned} C_{t,C}\delta C + C_{t,M}\delta M &= 0 && (25)\\ M_{t,C}\delta\dot{C} + M_{t,M}\delta\dot{M} &= \frac{1}{\tau_M}\Big(L_{,C}\delta C - M_{t,C}\delta C - M_{t,M}\delta M\Big), && (26)\end{aligned}$$

which results in

$$\begin{aligned} \delta\dot{C} &= \frac{1}{\tau_M}\,\frac{(L_{,C} - M_{t,C})C_{t,M} + M_{t,M}C_{t,C}}{M_{t,C}C_{t,M} - M_{t,M}C_{t,C}}\;\delta C \\ &= -\frac{1}{\tau_M}\,\frac{M_{t,M}}{A}\,\frac{\mathrm{d}CI_{\text{tot}}}{\mathrm{d}CI}\;\delta C, && (27)\end{aligned}$$

with the notation

$$A \equiv C_{t,C}M_{t,M} - C_{t,M}M_{t,C} > 0,$$

whose inequality can be shown from the actual expressions of $[CI]_{\text{tot}}$ and $[MOR]_{\text{tot}}$, (3) and (4).

Therefore, we have

$$\frac{\mathrm{d}CI_{\text{tot}}}{\mathrm{d}CI} < 0 \qquad \text{unstable}$$

$$\frac{\mathrm{d}CI_{\text{tot}}}{\mathrm{d}CI} > 0 \qquad \text{stable.}$$

5.2. Stability of genetic switch with PL and PR:

The growth rate ω is determined by the characteristic equation

$$\begin{vmatrix} \frac{1}{\tau_M}(L_{,C} - M_{t,C}) - M_{t,C}\,\omega, & -\frac{1}{\tau_M} M_{t,M} - M_{t,M}\,\omega \\ \frac{1}{\tau_C}(R_{,C} - C_{t,C}) - C_{t,C}\,\omega, & \frac{1}{\tau_C}(R_{,M} - C_{t,M}) - C_{t,M}\,\omega \end{vmatrix} = 0, \tag{28}$$

which can be expanded as

$$\begin{aligned} &\omega^2\left[M_{t,C}C_{t,M} - C_{t,C}M_{t,M}\right] \\ &+\omega\left[\frac{1}{\tau_C}\Big(-M_{t,C}(R_{,M} - C_{t,M}) + M_{t,M}(R_{,C} - C_{t,C})\Big) - \frac{1}{\tau_M}\Big(C_{t,M}(L_{,C} - M_{t,C}) + C_{t,C}M_{t,M}\Big)\right] \\ &+\frac{1}{\tau_M\tau_C}\left[(L_{,C} - M_{t,C})(R_{,M} - C_{t,M}) + (R_{,C} - C_{t,C})M_{t,M}\right] = 0. \end{aligned} \tag{29}$$

This can be put in the form

$$\begin{aligned} &-\omega^2\frac{A}{M_{t,M}} + \omega\left[\left\{\frac{1}{\tau_C}\left(\frac{\mathrm{d}\,pR}{\mathrm{d}CI} - \frac{\mathrm{d}\,CI_{\mathrm{tot}}}{\mathrm{d}CI}\right) - \frac{1}{\tau_M}\frac{\mathrm{d}\,CI_{\mathrm{tot}}}{\mathrm{d}CI}\right\} - \frac{1}{\tau_C}\frac{L_{,C}\big(R_{,M} - C_{t,M}\big)}{M_{t,M}}\right] \\ &+\frac{1}{\tau_M\tau_C}\left[\frac{\mathrm{d}\,pR}{\mathrm{d}CI} - \frac{\mathrm{d}\,CI_{\mathrm{tot}}}{\mathrm{d}CI}\right] = 0. \end{aligned} \tag{30}$$

This is almost the same with the corresponding equation for Model A eq.(20).

(1) The case of $\tau_M \ll \tau_C$. One solution is of order $1/\tau_M$ and the other of order $1/\tau_C$:

$$\omega \approx \begin{cases} -\dfrac{1}{\tau_M}\dfrac{M_{t,M}}{A}\left(\dfrac{\mathrm{d}CI_{\mathrm{tot}}}{\mathrm{d}CI}\right) \\ \dfrac{1}{\tau_C}\left[\dfrac{\mathrm{d}\,pR}{\mathrm{d}CI} - \dfrac{\mathrm{d}\,CI_{\mathrm{tot}}}{\mathrm{d}CI}\right]\left(\dfrac{\mathrm{d}CI_{\mathrm{tot}}}{\mathrm{d}CI}\right)^{-1} \end{cases}. \tag{31}$$

Therefore, the criterion (8) is valid as long as the slope of degradation curve is positive, i.e. $(\mathrm{d}CI_{\mathrm{tot}}/\mathrm{d}CI) > 0$, but the state is always unstable for the negative slope for the degradation curve, i.e. $(\mathrm{d}CI_{\mathrm{tot}}/\mathrm{d}CI) < 0$.

(2) The case of $\tau_C \ll \tau_M$.

$$\omega \approx \begin{cases} \dfrac{1}{\tau_C}\dfrac{M_{t,M}}{A}\left[\left(\dfrac{\mathrm{d}\,pR}{\mathrm{d}CI} - \dfrac{\mathrm{d}\,CI_{\mathrm{tot}}}{\mathrm{d}CI}\right) - \dfrac{L_{,C}\big(R_{,M} - C_{t,M}\big)}{M_{t,M}}\right] \\ -\dfrac{1}{\tau_M}\left[\left(\dfrac{\mathrm{d}\,pR}{\mathrm{d}CI} - \dfrac{\mathrm{d}\,CI_{\mathrm{tot}}}{\mathrm{d}CI}\right) - \dfrac{L_{,C}\big(R_{,M} - C_{t,M}\big)}{M_{t,M}}\right]^{-1}\left[\dfrac{\mathrm{d}\,pR}{\mathrm{d}CI} - \dfrac{\mathrm{d}\,CI_{\mathrm{tot}}}{\mathrm{d}CI}\right] \end{cases} \tag{32}$$

In this case, the criterion (8) is always valid because

$$\frac{L_{,C}\big(R_{,M} - C_{t,M}\big)}{M_{t,M}} > 0, \qquad \frac{M_{t,M}}{A} > 0.$$

(3) General case. We can show eq.(30) always has two real solutions, ω_1 and ω_2, and the steady state stability is determined from the sign of $\omega_1 + \omega_2$:

$$\frac{\mathrm{d}\,pR}{\mathrm{d}CI} - \frac{\mathrm{d}\,CI_{\mathrm{tot}}}{\mathrm{d}CI} < 0, \qquad \frac{\mathrm{d}\,CI_{\mathrm{tot}}}{\mathrm{d}CI} > 0 \quad \text{then stable}$$

$$\frac{\mathrm{d}\,pR}{\mathrm{d}CI} - \frac{\mathrm{d}\,CI_{\mathrm{tot}}}{\mathrm{d}CI} > 0, \qquad \qquad \text{then unstable}$$

but

$$\frac{\mathrm{d}\,pR}{\mathrm{d}CI} - \frac{\mathrm{d}\,CI_{\mathrm{tot}}}{\mathrm{d}CI} < 0, \qquad \frac{\mathrm{d}\,CI_{\mathrm{tot}}}{\mathrm{d}CI} < 0 \quad \text{stable/unstable.}$$

This means that *the stability cannot be determined only from the slopes of the production and the degradation curves in the case the degradation curve has a negative slope.*

Appendix: The positivity of the discriminant *D* of eq. (29):

$$\begin{aligned}
D \;=\;& \Bigg[\frac{1}{\tau_C}\Big(-M_{t,C}(R_{,M} - C_{t,M}) + M_{t,M}(R_{,C} - C_{t,C})\Big) \\
&\qquad\qquad -\frac{1}{\tau_M}\Big(C_{t,M}(L_{,C} - M_{t,C}) + C_{t,C}M_{t,M}\Big)\Bigg]^2 \\
&-\frac{4}{\tau_M\tau_C}\Big[M_{t,C}C_{t,M} - C_{t,C}M_{t,M}\Big]\Big[(L_{,C} - M_{t,C})(R_{,M} - C_{t,M}) + (R_{,C} - C_{t,C})M_{t,M}\Big] \\
=\;& \Bigg[\frac{1}{\tau_C}\Big(-A - R_{,M}M_{t,C} + R_{,C}M_{t,M}\Big) - \frac{1}{\tau_M}\Big(A + L_{,C}C_{t,M}\Big)\Bigg]^2 \\
&\qquad +\frac{4}{\tau_M\tau_C}A\Big[-A + L_{,C}R_{,M} - L_{,C}C_{t,M} - R_{,M}M_{t,C} + R_{,C}M_{t,M}\Big] \\
=\;& \Bigg[-A\Big(\frac{1}{\tau_C} + \frac{1}{\tau_M}\Big) + \Big(\frac{1}{\tau_C}(-R_{,M}M_{t,C} + R_{,C}M_{t,M}) - \frac{1}{\tau_M}L_{,C}C_{t,M}\Big)\Bigg]^2 \\
&\qquad +\frac{4}{\tau_M\tau_C}A\Big[-A + L_{,C}R_{,M} - L_{,C}C_{t,M} - R_{,M}M_{t,C} + R_{,C}M_{t,M}\Big] \\
=\;& A^2\left[\frac{1}{\tau_C} - \frac{1}{\tau_M}\right]^2 + 2A\Bigg[\Big(\frac{1}{\tau_C} + \frac{1}{\tau_M}\Big)\Big(\frac{1}{\tau_C}(R_{,M}M_{t,C} - R_{,C}M_{t,M}) + \frac{1}{\tau_M}L_{,C}C_{t,M}\Big) \\
&\qquad\qquad +\frac{2}{\tau_M\tau_C}\Big(L_{,C}R_{,M} - L_{,C}C_{t,M} - R_{,M}M_{t,C} + R_{,C}M_{t,M}\Big)\Bigg] \\
&\quad +\Big(\frac{1}{\tau_C}(-R_{,M}M_{t,C} + R_{,C}M_{t,M}) - \frac{1}{\tau_M}L_{,C}C_{t,M}\Big)^2
\end{aligned}$$

The coefficient of $2A$ is

$$\big(R_{,M}M_{t,C} - R_{,C}M_{t,M}\big)\Big(\frac{1}{\tau_C} - \frac{1}{\tau_M}\Big)\frac{1}{\tau_C} + L_{,C}C_{t,M}\Big(-\frac{1}{\tau_C} + \frac{1}{\tau_M}\Big)\frac{1}{\tau_M} + L_{,C}R_{,M}\frac{2}{\tau_M\tau_C},$$

$$= \left(\frac{1}{\tau_C} - \frac{1}{\tau_M}\right)\left(\frac{1}{\tau_C}(R_{,M}M_{t,C} - R_{,C}M_{t,M}) - \frac{1}{\tau_M}L_{,C}C_{t,M}\right) + \frac{2}{\tau_M\tau_C}L_{,C}R_{,M}.$$

Thus, D is

$$\begin{aligned}
D &= A^2\left(\frac{1}{\tau_C} - \frac{1}{\tau_M}\right)^2 \\
&\quad +2A\left[\left(\frac{1}{\tau_C} - \frac{1}{\tau_M}\right)\left(\frac{1}{\tau_C}(R_{,M}M_{t,C} - R_{,C}M_{t,M}) - \frac{1}{\tau_M}L_{,C}C_{t,M}\right) + \frac{2}{\tau_M\tau_C}L_{,C}R_{,M}\right] \\
&\qquad +\left(\frac{1}{\tau_C}(R_{,M}M_{t,C} - R_{,C}M_{t,M}) + \frac{1}{\tau_M}L_{,C}C_{t,M}\right)^2 \\
&= \left[\left(\frac{1}{\tau_C} - \frac{1}{\tau_M}\right)A + \left(\frac{1}{\tau_C}(R_{,M}M_{t,C} - R_{,C}M_{t,M}) - \frac{1}{\tau_M}L_{,C}C_{t,M}\right)\right]^2 \\
&\quad -\left(\frac{1}{\tau_C}(R_{,M}M_{t,C} - R_{,C}M_{t,M}) - \frac{1}{\tau_M}L_{,C}C_{t,M}\right)^2 + 2A\frac{2}{\tau_M\tau_C}L_{,C}R_{,M} \\
&\qquad +\left(\frac{1}{\tau_C}(R_{,M}M_{t,C} - R_{,C}M_{t,M}) + \frac{1}{\tau_M}L_{,C}C_{t,M}\right)^2 \\
&= \left[\left(\frac{1}{\tau_C} - \frac{1}{\tau_M}\right)A + \left(\frac{1}{\tau_C}(R_{,M}M_{t,C} - R_{,C}M_{t,M}) - \frac{1}{\tau_M}L_{,C}C_{t,M}\right)\right]^2 \\
&\quad +\frac{4}{\tau_C\tau_M}L_{,C}\Big(\big(R_{,M}M_{t,C} - R_{,C}M_{t,M}\big)C_{t,M} + \big(C_{t,C}M_{t,M} - C_{t,M}M_{t,C}\big)R_{,M}\Big)
\end{aligned}$$

The second line of the last expression is shown to be positive as follows:

Note that

$$C_{t,C} = 1 + C_{2,C} + MC_{,C}, \quad C_{t,M} = MC_{,M}, \quad M_{t,C} = MC_{,C}, \quad M_{t,M} = 1 + MC_{,C},$$

$$R_{,C} = R' \cdot MC_{,C}, \quad R_{,M} = R' \cdot MC_{,M},$$

where the abbreviated notations are used,

$$C_{2,C} \equiv \frac{\partial[CI_2]}{\partial[CI]}, \quad MC_{,M} \equiv \frac{\partial[MOR \cdot CI]}{\partial[MOR]}, \quad \text{etc. and} \quad R' \equiv \frac{\partial\, pR}{\partial[MOR \cdot CI]}.$$

Then the second line of D is

$$\begin{aligned}
&L_{,C}\Big(\big(R_{,M}M_{t,C} - R_{,C}M_{t,M}\big)C_{t,M} + \big(C_{t,C}M_{t,M} - C_{t,M}M_{t,C}\big)R_{,M}\Big) \\
&\quad = L_{,C}\big(-R_{,C}M_{t,M}C_{t,M} + C_{t,C}M_{t,M}R_{,M}\big) \\
&\quad = L_{,C}\, M_{t,M}(-R_{,C}C_{t,M} + R_{,M}C_{t,C}) \\
&\quad = L_{,C}\, M_{t,M}\big(-R' \cdot MC_{,C}MC_{,M} + R' \cdot MC_{,M}(1 + C_{2,C} + MC_{,C})\big) \\
&\quad = L_{,C}\, R' \cdot MC_{,M}(1 + C_{2,C}) > 0
\end{aligned}$$

Therefore,

$$D > 0.$$